

# Variational methods for Conditional Multimodal Learning: Generating Human Faces from Attributes

Gaurav Pandey and Ambedkar Dukkipati

Indian Institute of Science  
Bangalore, India

{gp88, ad}@csa.iisc.ernet.in

## Abstract

*Prior to this decade, the field of computer vision was primarily focused around hand-crafted feature extraction methods used in conjunction with discriminative models for specific tasks such as object recognition, detection/localization, tracking etc. A generative image understanding was neither within reach nor the prime concern of the period. In this paper, we address the following problem: Given a description of a human face, can we generate the image corresponding to it? We frame this problem as a conditional modality learning problem and use variational methods for maximizing the corresponding conditional log-likelihood. The resultant deep model, which we refer to as conditional multimodal autoencoder (CMMA), forces the latent representation obtained from the attributes alone to be ‘close’ to the joint representation obtained from both face and attributes. We show that the faces generated from attributes using the proposed model, are qualitatively and quantitatively more representative of the attributes from which they were generated, than those obtained by other deep generative models. We also propose a secondary task, whereby the existing faces are modified by modifying the corresponding attributes. We observe that the modifications in face introduced by the proposed model are representative of the corresponding modifications in attributes. Hence, our proposed method solves the above mentioned problem.*

## 1. Introduction

In 2006, Hinton and his collaborators [10] made the observation that generative models are capable of learning Gabor-like filters from images of characters. Not only was it possible to sample MNIST-like characters from these models, the learned representations could also be discriminatively fine-tuned to improve the classification performance on MNIST characters. Though this spurred an interest in models for unsupervised learning, the prime focus still re-

mained the achievement of improved performance on discriminative tasks [20, 6]. It is only in the recent years, that, achieving a deeper image understanding, which subsumes the capability to generate realistic images, has started gaining interest. Several generative models that build upon the models for unsupervised learning of the previous decade have been proposed[22, 1, 8, 15, 2].

In this paper, we attempt to solve the problem of generating faces given the set of attributes/tags that the face must possess. One can think of images and attributes as two modalities of the data [19, 23]. The first instinct to approach this problem is to train a neural network from the attributes to the faces. This will force the images generated from attributes to be close in image-space (in terms of mean-squared error) to the actual image that corresponds to the attributes. To keep things in perspective, assume that we have only one attribute, say the ‘moustache’ attribute and we train the model. If we generate a face with moustache from the trained model, it will be an average in image-space over all faces that contain a moustache. This is certainly undesirable, since an average in image-space need not correspond to a meaningful image at all. Another disadvantage of this model is its unidirectional nature. For instance, if we wish to modify the attributes of an already existing face (say, add a moustache), we can not achieve the same using a deterministic neural network.

Hence, we resort to a probabilistic model. Given enough training examples, it is theoretically possible to learn a joint distribution over the faces and the attributes. However, since we are only interested in generating faces from attributes, it is reasonable to learn a conditional distribution on the faces given the attributes directly, rather than inferring it from the joint distribution. Also referred to as conditional learning [12], this method of learning has been immensely successful for several tasks that include, but are not limited to, natural language processing [3], computer vision [9, 26] etc. It is based on the principle that “one should always solve the problem directly and not solve a more general problem as an intermediate step” [25, 18].

Since the conditional log-likelihood of the proposed model is intractable, we use variational methods for training the model, whereby the posterior of the latent variables given the faces and the attributes is approximated by a tractable distribution. While variational methods have long been a popular tool for training graphical models, their usage for deep learning became popular after the reparametrization trick of [15, 21, 24]. Prior to that, mean-field approximation has been used for training deep Boltzmann machines (DBM) [22]. However, the training of DBM involves solving a variational approximation problem for every instance in the training data. On the other hand, reparametrizing the posterior allows one to single parametrized variational approximation problem for all instances in the training data simultaneously.

The proposed model is referred to as conditional multimodal autoencoder (CMMA). We use CMMA for the task of generating faces from attributes, and to modify faces in the training data, by modifying the corresponding attributes. The dataset used is the cropped Labelled Faces in the Wild dataset<sup>1</sup> (LFW) [11]. We also compare the qualitative and quantitative performance of CMMA against other models that are capable of generating faces from tags/attributes. These include conditional generative adversarial networks (CGAN) [17, 7] and conditional variational autoencoder (CVAE) [13]. More information about these models is provided in Section 3.

The main contributions of this paper are as follows:

1. We frame the problem of generating faces from attributes as a conditional modality learning problem, whereby faces are generated by sampling a latent layer conditioned on the attributes, and then sampling the faces conditioned on the latent layer.
2. We derive the variational lower bound of the conditional log-likelihood, and use stochastic backpropagation [21] (also known as SGVB [15]) to optimize this lower bound.
3. We use the proposed model for generating faces from attributes and modifying faces in the training data for the Labelled Faces in the Wild (LFW) dataset.
4. We show that the proposed model is quantitatively and qualitatively superior to CGAN [17, 7] and CVAE [13] for the proposed task.

## 2. Problem Formulation and Proposed Solution

We formulate the problem as a multimodal learning problem whereby the face corresponds to the modality that

<sup>1</sup>The dataset is available at <http://conradsanderson.id.au/lfwcrop/>

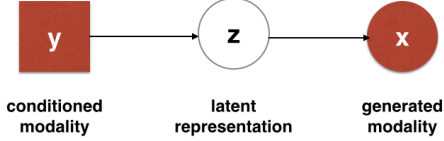


Figure 1: A graphical representation of CMMA

we wish to generate and the attributes correspond to the modality that we wish to condition on.

A formal description of the problem is as follows. We are given an *i.i.d* sequence of  $N$  datapoints  $\{(\mathbf{x}^{(1)}, \mathbf{y}^{(1)}), \dots, (\mathbf{x}^{(N)}, \mathbf{y}^{(N)})\}$ . For a fixed datapoint  $(\mathbf{x}, \mathbf{y})$ , let  $\mathbf{x}$  be the modality that we wish to generate and  $\mathbf{y}$  be the modality that we wish to condition on. We assume that  $\mathbf{x}$  is generated by first sampling a real-valued latent representation  $\mathbf{z}$  from the distribution  $p(\mathbf{z}|\mathbf{y})$ , and then sampling  $\mathbf{x}$  from the distribution  $p(\mathbf{x}|\mathbf{z})$ . The graphical representation of the model is given in Figure 1. Furthermore, we assume that the conditional distribution of the latent representation  $\mathbf{z}$  given  $\mathbf{y}$  and the distribution of  $\mathbf{x}$  given  $\mathbf{z}$  are parametric.

Given the above description of the model, our aim is to find the parameters so as maximize the conditional log-likelihood of  $\mathbf{x}$  given  $\mathbf{y}$  for the given sequence of datapoints. The computation of conditional log-likelihood requires the marginalization of the latent variable  $\mathbf{z}$  from the joint distribution  $p(\mathbf{x}, \mathbf{z}|\mathbf{y})$ .

$$p(\mathbf{x}|\mathbf{y}) = \int p(\mathbf{x}, \mathbf{z}|\mathbf{y}) d\mathbf{z} \quad (1)$$

$$= \int p(\mathbf{x}|\mathbf{z}) p(\mathbf{z}|\mathbf{y}) d\mathbf{z} \quad (2)$$

For most choices of  $p(\mathbf{x}|\mathbf{z})$  and  $p(\mathbf{z}|\mathbf{y})$ , the evaluation of conditional log-likelihood is intractable. Hence, we resort to the minimization of a variational lower bound to the conditional log-likelihood. This is achieved by approximating the posterior distribution of  $\mathbf{z}$  given  $\mathbf{x}$  and  $\mathbf{y}$ , that is  $p(\mathbf{z}|\mathbf{x}, \mathbf{y})$  by a tractable distribution  $q(\mathbf{z}|\mathbf{x}, \mathbf{y})$ . This is explained in more detail in the following section.

### 2.1. The variational bound

For a given *i.i.d* collection of datapoints,  $\{(\mathbf{x}^{(1)}, \mathbf{y}^{(1)}), \dots, (\mathbf{x}^{(N)}, \mathbf{y}^{(N)})\}$ , the conditional log-likelihood can be written as

$$\begin{aligned} \log p(\mathbf{x}^{(1)}, \dots, \mathbf{x}^{(N)} | \mathbf{y}^{(1)}, \dots, \mathbf{y}^{(N)}) \\ = \sum_{i=1}^N \log p(\mathbf{x}^{(i)} | \mathbf{y}^{(i)}) \end{aligned} \quad (3)$$

Distribution	Parametric form	Representation
$p(\mathbf{z} \mathbf{y})$	$\mathcal{N}(f_\mu(\mathbf{y}), e^{f_\sigma(\mathbf{y})})$	$p_f(\mathbf{z} \mathbf{y})$
$p(\mathbf{x} \mathbf{z})$	$\mathcal{N}(g_\mu(\mathbf{z}), e^{g_\sigma(\mathbf{z})})$	$p_g(\mathbf{x} \mathbf{z})$
$q(\mathbf{z} \mathbf{x}, \mathbf{y})$	$\mathcal{N}(h_\mu(\mathbf{x}, \mathbf{y}), e^{h_\sigma(\mathbf{x}, \mathbf{y})})$	$q_h(\mathbf{z} \mathbf{x}, \mathbf{y})$

Table 1: Parametric forms for the distributions used in the paper and their representations demonstrating the explicit dependence on  $f$ ,  $g$  and  $h$ .

Let  $q(\mathbf{z}|\mathbf{x}, \mathbf{y})$  be an approximation to the posterior distribution of the latent variables given  $\mathbf{x}$  and  $\mathbf{y}$ . For an individual datapoint, this conditional log-likelihood can be rewritten as

$$\begin{aligned} & \log p(\mathbf{x}|\mathbf{y}) \\ &= \mathbb{E}_{q(\mathbf{z}|\mathbf{x}, \mathbf{y})} \log \frac{p(\mathbf{x}, \mathbf{z}|\mathbf{y})}{p(\mathbf{z}|\mathbf{x}, \mathbf{y})} \end{aligned} \quad (4)$$

$$\begin{aligned} &= \text{KL}[q(\cdot|\mathbf{x}, \mathbf{y})||p(\cdot|\mathbf{x}, \mathbf{y})] + \mathbb{E}_{q(\mathbf{z}|\mathbf{x}, \mathbf{y})} \log \frac{p(\mathbf{x}, \mathbf{z}|\mathbf{y})}{q(\mathbf{z}|\mathbf{x}, \mathbf{y})} \\ &\geq \mathbb{E}_{q(\mathbf{z}|\mathbf{x}, \mathbf{y})} \log \frac{p(\mathbf{x}, \mathbf{z}|\mathbf{y})}{q(\mathbf{z}|\mathbf{x}, \mathbf{y})}, \end{aligned} \quad (5)$$

where  $\text{KL}(p||q)$  refers to the KL-divergence between the distributions  $p$  and  $q$  and is always non-negative. The term in equation (5) is referred to as the variational lower bound for the conditional log-likelihood for the datapoint  $(\mathbf{x}, \mathbf{y})$  and will be denoted by  $\mathcal{L}(p, q; \mathbf{x}, \mathbf{y})$ . It can further be rewritten as

$$\begin{aligned} & \mathcal{L}(p, q; \mathbf{x}, \mathbf{y}) \\ &= \mathbb{E}_{q(\mathbf{z}|\mathbf{x}, \mathbf{y})} \log p(\mathbf{x}|\mathbf{z}) + \mathbb{E}_{q(\mathbf{z}|\mathbf{x}, \mathbf{y})} \log \frac{p(\mathbf{z}|\mathbf{y})}{q(\mathbf{z}|\mathbf{x}, \mathbf{y})} \\ &= \mathbb{E}_{q(\mathbf{z}|\mathbf{x}, \mathbf{y})} \log p(\mathbf{x}|\mathbf{z}) - \text{KL}[q(\mathbf{z}|\mathbf{x}, \mathbf{y})||p(\mathbf{z}|\mathbf{y})] \end{aligned} \quad (6)$$

From the last equation, we observe that the variational lower bound can be written as the sum of two terms. The first term is the negative of reconstruction error of  $\mathbf{x}$ , when reconstructed from the joint encoding  $\mathbf{z}$  of  $\mathbf{x}$  and  $\mathbf{y}$ . The second term ensures that the joint encoding of  $\mathbf{x}$  and  $\mathbf{y}$  is 'close' to the encoding of  $\mathbf{y}$  alone, where closeness is defined in terms of KL-divergence between the corresponding distributions.

## 2.2. The reparametrization

In order to simplify the computation of the variational lower bound, we assume that conditioned on  $\mathbf{y}$ , the latent representation  $\mathbf{z}$  is normally distributed with mean  $f_\mu(\mathbf{y})$  and a diagonal covariance matrix whose diagonal entries are given by  $e^{f_\sigma(\mathbf{y})}$ . Moreover, conditioned on  $\mathbf{z}$ ,  $\mathbf{x}$  is normally distributed with mean  $g_\mu(\mathbf{z})$  and a diagonal covariance matrix whose diagonal entries are given by  $e^{g_\sigma(\mathbf{y})}$ . In

the rest of the paper, we assume  $f_\mu, f_\sigma, g_\mu$  and  $g_\sigma$  to be multi-layer perceptrons. Furthermore, we approximate the posterior distribution of  $\mathbf{z}$  given  $\mathbf{x}$  and  $\mathbf{y}$  by a normal distribution with mean  $h_\mu(\mathbf{x}, \mathbf{y})$  and a diagonal covariance matrix whose diagonal entries are given by  $e^{h_\sigma(\mathbf{x}, \mathbf{y})}$ , where  $h_\mu$  and  $h_\sigma$  are again multi-layer perceptrons. In order to make the dependence of the distributions on  $f$ ,  $g$  and  $h$  explicit, we represent  $p(\mathbf{z}|\mathbf{y})$  as  $p_f(\mathbf{z}|\mathbf{y})$ ,  $p(\mathbf{x}|\mathbf{z})$  as  $p_g(\mathbf{x}|\mathbf{z})$  and  $q(\mathbf{z}|\mathbf{x}, \mathbf{y})$  as  $q_h(\mathbf{z}|\mathbf{x}, \mathbf{y})$ . For reference, the parametric forms of the likelihood, prior and posterior distributions and their representations demonstrating the explicit dependence on  $f$ ,  $g$  and  $h$  are given in Table 1.

The above assumptions simplify the calculation of KL-divergence and  $\log p(\mathbf{x}|\mathbf{z})$ . Let  $f_j$  denote the  $j^{th}$  component of the function  $f$  and the size of the latent representation be  $J$ . After ignoring the constant terms, the KL-divergence term of the variational lower bound can be written as

$$\begin{aligned} & \text{KL}(q_h(\mathbf{z}|\mathbf{x}, \mathbf{y})||p_f(\mathbf{z}|\mathbf{y})) = \\ & \frac{1}{2} \sum_{j=1}^J \left[ f_{j\sigma}(\mathbf{y}) - h_{j\sigma}(\mathbf{x}, \mathbf{y}) + \exp(h_{j\sigma}(\mathbf{x}, \mathbf{y}) - f_{j\sigma}(\mathbf{y})) \right. \\ & \quad \left. + \frac{(h_{j\mu}(\mathbf{x}, \mathbf{y}) - f_{j\mu}(\mathbf{y}))^2}{\exp(f_{j\sigma}(\mathbf{y}))} \right] \end{aligned} \quad (7)$$

The negative reconstruction error term in the variational lower bound in (6) can be obtained by generating samples from the posterior distribution of  $\mathbf{z}$  given  $\mathbf{x}$  and  $\mathbf{y}$ , and then averaging over the negative reconstruction error. For a fixed  $\mathbf{z}$ , the term can be written as

$$\log p_g(\mathbf{x}|\mathbf{z}) = - \left[ \sum_{l=1}^m \frac{(g_{l\mu}(\mathbf{z}) - \mathbf{x}_l)^2}{2 \exp(g_{l\sigma})} + \sum_{l=1}^m \exp(g_{l\sigma}(\mathbf{z})) \right] \quad (8)$$

The choice of the posterior allows us to sample  $\mathbf{z}$  as follows:

$$\epsilon \sim \mathcal{N}(0, I) \quad (9)$$

$$\mathbf{z} = h_\mu(\mathbf{x}, \mathbf{y}) + \epsilon \odot h_\sigma(\mathbf{x}, \mathbf{y}) \quad (10)$$

where  $\odot$  denotes elementwise multiplication. Hence, the negative reconstruction error can alternatively be rewritten as

$$\mathbb{E}_{\epsilon \sim \mathcal{N}(0, I)} \log p_g(\mathbf{x}|h_\mu(\mathbf{x}, \mathbf{y}) + \epsilon \odot h_\sigma(\mathbf{x}, \mathbf{y})), \quad (11)$$

where  $\log p_g(\mathbf{x}|\cdot)$  is as defined in (8)

In order to train the model using first-order methods, we need to compute the derivative of the variational lower bound with respect to the parameters of the model. Let  $\theta_f$ ,  $\theta_g$  and  $\theta_h$  be the parameters of  $\{f_\mu, f_\sigma\}$ ,  $\{g_\mu, g_\sigma\}$  and  $\{h_\mu, h_\sigma\}$  respectively. Note that the KL-divergence term in (7) depends only on  $\{f_\mu, f_\sigma\}$ , and  $\{h_\mu, h_\sigma\}$ . Its derivatives with respect to  $\theta_f$  and  $\theta_h$  can be computed via chain rule.

From (11), the derivative of the negative reconstruction error with respect to  $\{\theta_g, \theta_h\}$  is given by

$$\mathbb{E}_{\epsilon \sim \mathcal{N}(0, I)} \nabla_{\{\theta_g, \theta_h\}} \log p_g(\mathbf{x} | h_\mu(\mathbf{x}, \mathbf{y}) + \epsilon \odot h_\sigma(\mathbf{x}, \mathbf{y})) \quad (12)$$

The term inside the expectation can again be evaluated using chain rule.

### 2.3. Implementation details

We use minibatch training to learn the parameters of the model, whereby the gradient of the model with respect to the model parameters  $\{\theta_f, \theta_g, \theta_h\}$  is computed for every minibatch and the corresponding parameters updated. While the gradient of the KL-divergence can be computed exactly from (7), the gradient of the negative reconstruction error in (11) requires one to sample standard normal random vectors, compute the gradient for each sampled vector, and then take the mean. In practise, when the minibatch size is large enough, it is sufficient to sample one standard normal random vector per training example, and then compute the gradient of the negative reconstruction error with respect to the parameters, for this vector. This has also been observed for the case of variational autoencoder in [15].

A pictorial representation of the implemented model is given in Figure 2. Firstly,  $\mathbf{x}$  and  $\mathbf{y}$  are fed to the neural network  $h$  to generate mean and log-variance of the distribution  $q_h(\mathbf{z} | \mathbf{x}, \mathbf{y})$ . Moreover,  $\mathbf{y}$  is fed to the neural network  $f$  to generate the mean and log-variance of the distribution  $p_f(\mathbf{z} | \mathbf{y})$ . The KL-divergence between  $q_h(\mathbf{z} | \mathbf{x}, \mathbf{y})$  and  $p_f(\mathbf{z} | \mathbf{y})$  is computed using (7), and its gradient is backpropagated to update the parameters  $\theta_f$  and  $\theta_h$ . Furthermore, the mean and log-variance of  $q_h(\mathbf{z} | \mathbf{x}, \mathbf{y})$  are used to sample  $\mathbf{z}$ , which is then forwarded to the neural network  $g$  to compute the mean and log-variance of the distribution  $p_g(\mathbf{x} | \mathbf{z})$ . Finally, the negative reconstruction error is computed using equation (8) for the specific  $\mathbf{z}$  and its gradient is backpropagated to update the parameters  $\theta_g$  and  $\theta_h$ .

## 3. Related Works

Over the past few years, several deep generative models have been proposed. They include deep Boltzmann machines (DBM) [22], generative adversarial networks (GAN) [8], variational autoencoders (VAE) [15] and generative stochastic networks (GSN) [1].

DBMs learn a Markov random field with multiple latent layers, and have been effective in modelling MNIST and NORB data. However, the training of DBMs involves a mean-field approximation step for every instance in the training data, and hence, they are computationally expensive. Moreover, there are no tractable extensions of deep Boltzmann machines for handling spatial equivariance.

All the other models mentioned above, can be trained using backpropagation or its stochastic variant, and hence can

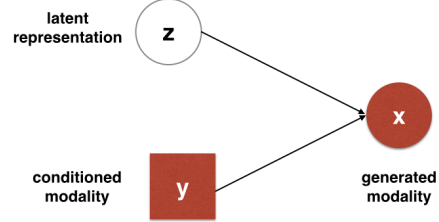


Figure 3: A graphical representation of conditional VAE as well as conditional GAN

incorporate the recent advances in training deep neural networks such as faster libraries and better optimization methods. In particular, GAN learns a distribution on data, by forcing the generator to generate samples that are ‘indistinguishable’ from training data. This is achieved by learning a discriminator whose task is to distinguish between the generated samples and samples in the training data. The generator is then trained to fool the discriminator. Though this approach is intuitive, it requires a careful selection of hyperparameters. Moreover, given the data, one can not sample the latent variables from which it was generated, since the posterior is never learnt by the model.

In a VAE, the posterior distribution of the latent variables conditioned on the data, is approximated by a normal distribution, whose mean and variance are the output of a neural network (distributions other than normal can also be used). This allows approximate estimation of variational log-likelihood which can be optimized using stochastic backpropagation [21].

Both GAN and VAE are directed probabilistic models with an edge from the latent layer to the data. Conditional extensions of both these models for incorporating attributes/labels have also been proposed [14, 7, 17]. The graphical representation of a conditional GAN or conditional VAE is shown in Figure 3. As can be observed, both these models assume the latent layer to be independent of the attributes/labels. This is in stark contrast with our model CMMA, which assumes that the latent layer is sampled conditioned on the attributes.

It is also informative to compare the variational lower bound of conditional log-likelihood for a CVAE with (6). The lower bound for a CVAE is given by

$$\log p(\mathbf{x} | \mathbf{y}) \geq \mathbb{E}_{q(\mathbf{z} | \mathbf{x}, \mathbf{y})} \log p(\mathbf{x} | \mathbf{y}, \mathbf{z}) - \text{KL}(q(\mathbf{z} | \mathbf{x}, \mathbf{y}) || p(\mathbf{z})) \quad (13)$$

Note that while the lower bound in the proposed model CMMA contains a KL-divergence term to explicitly force the latent representation from  $\mathbf{y}$  to be ‘close’ to the latent representation from both  $\mathbf{x}$  and  $\mathbf{y}$ , there is no such term in the lower bound of CVAE. This proves to be a disadvantage for CVAE as is reflected in the experiments section.

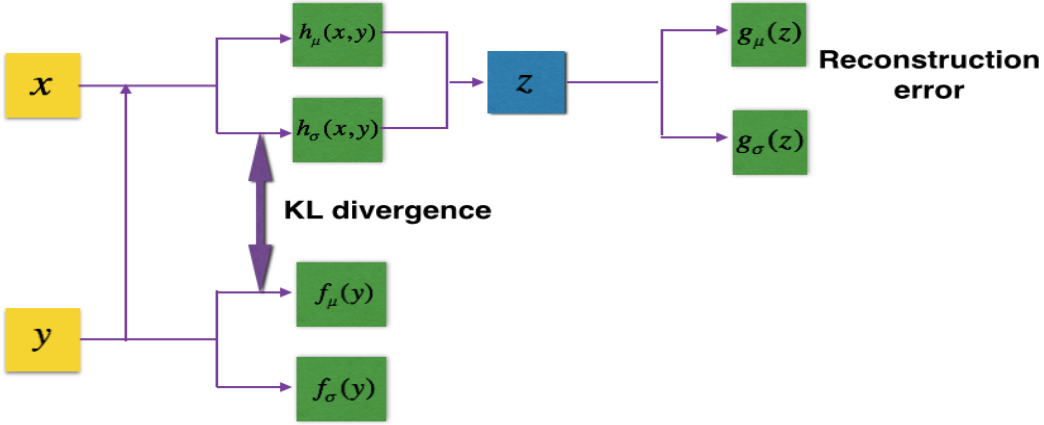


Figure 2: A pictorial representation of the implemented model. The KL-divergence between  $q_h(z|x, y)$  and  $p_f(z|y)$  is computed using (7) and backpropagated to update the parameters  $\theta_h$  and  $\theta_f$ . Similarly, the negative reconstruction error is computed using equation (8) for the specific  $z$  and its gradient is backpropagated to update the parameters  $\theta_g$  and  $\theta_h$ .

## 4. Experiments

For our experiments, we use the cropped Labelled Faces in the Wild dataset<sup>2</sup> (LFW) [11], which consists of 13,233 faces of 5749 people of which 4069 people have only one image. The images are of size  $64 \times 64$  and contain 3 channels (red green and blue). Of the 13,233 faces, 13,143 faces have 73 attributes associated with them, obtained partially using Amazon Mechanical Turk and partially using attribute classifiers [16]. The attributes include ‘Male’, ‘Asian’, ‘No eye-wear’, ‘Eyeglasses’, ‘Moustache’, ‘Mouth open’, ‘Big nose’, ‘Pointy nose’, ‘Smiling’, ‘Frowning’, ‘Big lips’ etc. The data also contains attributes for hair, necklace, earrings etc., though these attributes are not visible in the cropped images. We use the first 10,000 faces and the corresponding 73 attributes for training the model, the next 1000 faces for validation, and keep the remaining faces and their corresponding attributes for testing.

### 4.1. CMMA architecture

The MLP  $\{f_\mu, f_\sigma\}$  of the CMMA used in this paper (refer Figure 2) encodes the attributes, and is a neural network with 800 hidden units, a soft thresholding unit of the form  $\log(1 + e^x)$  and two parallel output layers, each comprising of 500 units. The MLP  $\{h_\mu, h_\sigma\}$  is a convolutional neural network, and comprises of the following layers:

1. Three convolutional layers with 192 filters of size  $3 \times 5 \times 5$ , 96 filters of size  $192 \times 5 \times 5$  and 48 filters of size  $96 \times 4 \times 4$  in the first, second and third convolutional layers respectively.
2. A  $2 \times 2$  max-pooling layer after the first and second

<sup>2</sup>The dataset is available at <http://conradsanderson.id.au/lfwcrop/>

convolutional layer.

3. A non-negative rectification layer after every max-pooling layer.
4. A non-negative rectification layer after the last convolutional layer.
5. Two parallel linear layers that maps the output of the last rectification layer to two output layers of size 500.

Note that, we do not explicitly feed the attributes to the MLP  $\{h_\mu, h_\sigma\}$ , since we did not observe any improvement in performance when the attributes were fed to the MLP  $\{h_\mu, h_\sigma\}$ . The MLP  $\{g_\mu, g_\sigma\}$  is a deconvolutional network and comprises of the following layers:

1. A linear layer that maps the latent representation  $z$  to 4800 dimensions and a reshaping layer to reshape it to 48 feature maps of size  $10 \times 10$ .
2. Two convolutional layers with 96 filters of size  $48 \times 3 \times 3$  and 192 filters of size  $96 \times 3 \times 3$  in the first and second convolutional layers respectively.
3. A  $2 \times 2$  nearest neighbour upsampling layer before every convolutional layer.
4. A non-negative rectification layer after the first two convolutional layer.
5. Two parallel convolutional layers at the output with 192 filters of size  $3 \times 5 \times 5$ . The first convolutional layer at the output is followed by a sigmoid non-linearity.

Model	Variational Lower Bound
<b>CMMA</b>	<b>17,973</b>
CVAE	14,356

Table 2: Variational lower bound to the conditional log-likelihood for the models CMMA and CVAE (Higher means better).

## 4.2. Models used for comparison

We compare the quantitative and qualitative performance of CMMA against conditional Generative Adversarial Networks [17, 7] (CGAN) and conditional Variational Autoencoders [15] (CVAE). We have tried to ensure that the architecture of the models used for comparison is as close as possible to the architecture of the CMMA used in our experiments. Hence, the generator and discriminator of CGAN and the encoder and decoder of CVAE closely mimic the MLPs  $g$  and  $h$  of CMMA as described in the previous section.

## 4.3. Training

We coded all the models in Torch [4] and trained each of them for 500 iterations on a Tesla K40 GPU. For each model, the training time was approximately 1 day. The adagrad optimization algorithm was used [5]. The proposed model CMMA was found to be relatively stable to the selection of initial learning rate, and the variance of the randomly initialized weights in various layers. For CGAN, we selected the learning rate of generator and discriminator and the variance of weights by verifying the conditional log-likelihood on the validation set. Only the results from the best hyperparameters have been reported. We found the CGAN model to be quite unstable to the selection of hyperparameters.

## 4.4. Quantitative results

For the first set of experiments, we compare the conditional log-likelihood of the faces given the attributes on the test set for the 3 models - CMMA, CGAN, and CVAE. A direct evaluation of conditional log-likelihood is infeasible, and for the size of latent layer used in our experiments (500), MCMC estimates of conditional log-likelihood are unreliable.

For the proposed model CMMA, a variational lower bound to the log-likelihood of the test data can be computed as the difference between the negative reconstruction error and KL-divergence (see (5)). The same can also be done for the CVAE model using (13). The corresponding values are provided in Table 2.

Since we can not obtain the variational lower bound for the other models, we use Parzen-window based log-likelihood estimation method for comparing the 3 models.

Model	Conditional Log-likelihood
<b>CMMA</b>	<b>9,487</b>
CVAE	8,714
CGAN	8,320

Table 3: Parzen window based estimates of conditional log-likelihood for the test data (Higher means better).

In particular, for a fixed test instance, we condition on the attributes to generate samples from the 3 models. A Gaussian Parzen window is fit to the generated samples, and the log-probability of the face in the test instance is computed for the obtained Gaussian Parzen window. The  $\sigma$ -parameter of the Parzen window estimator is obtained via cross-validation on the validation set. The corresponding log-likelihood estimates for the 3 models are given in Table 3.

In both the cases, the proposed model CMMA was able to achieve a better conditional log-likelihood than the other models.

## 4.5. Qualitative results

While the quantitative results do convey a sense of superiority of the proposed model over the other models used in comparison, it is more convincing to look at the actual samples generated by these models. Hence, we compare the three models CGAN, CVAE and CMMA for the task of generating faces from attributes. We also compare the two models CVAE and CMMA for modifying an existing face by changing the attributes. CGAN can not be used for modifying faces because of the uni-directional nature of the model, that is, it is not possible to sample the latent layer from an image in a generative adversarial network.

### 4.5.1 Generating faces from attributes

In our first set of experiments, we generate samples from the attributes using the 3 already trained models. In a CGAN, the images are generated by feeding noise and attributes to the generator. Similarly, in a CVAE, noise and attributes are fed to the MLP that corresponds to  $p(\mathbf{x}|\mathbf{z}, \mathbf{y})$  (see (13)) to sample the images. In order to generate images from attributes in a CMMA, we prune the MLP  $\{h_\mu, h_\sigma\}$  from the CMMA model (refer Figure 2), and connect the MLP  $\{f_\mu, f_\sigma\}$  in its stead as shown in Figure 5.

We set/reset the 'Male' and 'Asian' attributes to generate four possible combinations. The faces are then generated by varying the other attributes one at a time. In order to remove any bias from the selection of images, we set the variance parameter of the noise level to 0 in CMMA, CVAE and CGAN. The corresponding faces for our model CMMA, and the other models (CVAE [14] and CGAN [7])



(a) Faces generated from our model CMMA.



(b) Faces generated from CVAE [14].



(c) Faces generated from CGAN [7] using the hyperparameters selected by us.



(d) Faces generated from CGAN [7] using the hyperparameters used in [7].

Figure 4: Faces generated from the attributes using various models (Best viewed in color). For a fixed model, the 4 rows correspond to ‘Female Asian’, ‘Female Not-Asian’, ‘Male Asian’ and ‘Male Not-Asian’ in order. The remaining attributes are varied one at a time to generate the 7 columns. In particular, for each model, the 7 columns of faces correspond to i) no change, ii) mouth open, iii) spectacles, iv) bushy eyebrows, v) big nose ,vi) pointy nose and vii) thick lips. Note that, for our model CMMA, any change in attributes, such as mouth open, spectacles etc., is clearly reflected in the corresponding face. For other models, this change is not very evident from the corresponding faces.

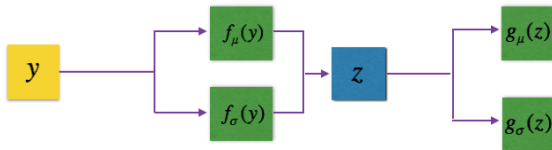


Figure 5: The model used for generating faces from attributes in CMMA is obtained by removing the MLP  $\{h_\mu, h_\sigma\}$  from the CMMA model (refer Figure 2), and connecting the MLP  $\{f_\mu, f_\sigma\}$  in its stead.

are listed in Figure 4. We have also presented the results from the implementation of CGAN<sup>3</sup> by the author of [7], since the images sampled from CGAN trained by us were quite noisy.

The 7 columns of images for each model correspond to the attributes i) no change, ii) mouth open, iii) specta-

cles, iv) bushy eyebrows, v) big nose ,vi) pointy nose and vii) thick lips. As is evident from the first image in Figure 4, CMMA can incorporate any change in attribute such as ‘open mouth’ or ‘spectacles’ in the corresponding face for each of the 4 rows. However, this does not seem to be the case for the other models. We hypothesize that this is because our model explicitly minimizes the KL-divergence between the latent representation of attributes and the joint representation of face and attributes.

#### 4.5.2 Varying the attributes in existing faces

In our next set of experiments, we select a face from the training data, and vary the attributes to generate a modified face. For a CMMA, this can be achieved as follows (also refer Figure 2):

1. Let  $attr_{orig}$  be the original attributes of the face and  $attr_{new}$  be the new attributes that we wish the face to possess.

<sup>3</sup><https://github.com/hans/adversarial>



(a) Modifying faces with CMMA



(b) Modifying faces with CVAE

Figure 6: Modifying the faces in the training data by modifying the corresponding attributes using CMMA and CVAE respectively (Best viewed in color). The rows in each of the above figures correspond to i) No change, ii) Big Nose, iii) Spectacles, iv) Moustache and v) Big lips. Except for spectacles, any other change in attributes is not reflected in the faces modified by CVAE.

2. Pass the selected face and the  $attr\_new$  through the MLP  $\{h_\mu, h_\sigma\}$ .
3. Pass  $attr\_orig$  and  $attr\_new$  through the MLP  $\{f_\mu, f_\sigma\}$  and compute the difference.
4. Add the difference to the output of MLP  $\{h_\mu, h_\sigma\}$ .
5. Pass the resultant sum through the decoder  $\{g_\mu, g_\sigma\}$ .

As in the previous case, we have the set the variance parameter of noise level to 0.

Note that, we can not use CGAN for this set of experiments, since, given a face, it is not possible to sample the latent layer in a CGAN. Hence, we only present the results



(a) Unchanged image



(b) After removal of spectacles with CMMA



(c) After removal of spectacles with CVAE

Figure 7: Removal of spectacles with CMMA and CVAE (Best viewed in color). The resultant eyes look more natural in case of CMMA than CVAE.

corresponding to our model CMMA and CVAE. The corresponding transformed faces are given in Figure 6a and Figure 6b respectively. As can be observed, for most of the attributes, our model, CMMA, is successfully able to transform images by removing moustaches, adding spectacles and making the nose bigger or pointy etc. However, some transformations such as addition of moustaches (4<sup>th</sup> row of Figure 6a) also create the impression of an open mouth, thereby suggesting that the latent representation of an open-mouth is correlated with the latent representation for a moustache.

Some more comparative experimental results are given in the supplementary.

## 5. Concluding Remarks

In this paper, we proposed a model for generating faces from attributes/tags, that forces the latent representation of attributes to be ‘close’ to the joint representation for face and attributes. Quantitative and qualitative results suggest that our model is more suitable for this task than CGAN [7] and CVAE [14]. Moreover, for the task of modifying faces, by modifying the attributes, CMMA does an arguably better job than CVAE.

## References

- [1] Y. Bengio, E. Thibodeau-Laufer, G. Alain, and J. Yosinski. Deep generative stochastic networks trainable by backprop. In *Proceedings of The 31st International Conference on Machine Learning*, pages 226–234.
- [2] Y. Bengio, L. Yao, G. Alain, and P. Vincent. Generalized denoising auto-encoders as generative models. In C. Burges, L. Bottou, M. Welling, Z. Ghahramani, and K. Weinberger, editors, *Advances in Neural Information Processing Systems 26*, pages 899–907. Curran Associates, Inc., 2013.

[3] A. L. Berger, V. J. D. Pietra, and S. A. D. Pietra. A maximum entropy approach to natural language processing. *Computational linguistics*, 22(1):39–71, 1996.

[4] R. Collobert, K. Kavukcuoglu, and C. Farabet. Torch7: A matlab-like environment for machine learning. In *BigLearn, NIPS Workshop*, number EPFL-CONF-192376, 2011.

[5] J. Duchi, E. Hazan, and Y. Singer. Adaptive subgradient methods for online learning and stochastic optimization. *The Journal of Machine Learning Research*, 12:2121–2159, 2011.

[6] D. Erhan, Y. Bengio, A. Courville, P.-A. Manzagol, P. Vincent, and S. Bengio. Why does unsupervised pre-training help deep learning? *The Journal of Machine Learning Research*, 11:625–660, 2010.

[7] J. Gauthier. Conditional generative adversarial nets for convolutional face generation.

[8] I. Goodfellow, J. Pouget-Abadie, M. Mirza, B. Xu, D. Warde-Farley, S. Ozair, A. Courville, and Y. Bengio. Generative adversarial nets. In *Advances in Neural Information Processing Systems*, pages 2672–2680, 2014.

[9] X. He, R. S. Zemel, and M. Á. Carreira-Perpiñán. Multiscale conditional random fields for image labelling. In *IEEE Conference on Computer Vision and Pattern Recognition*, volume 2, pages II–695. IEEE, 2004.

[10] G. E. Hinton, S. Osindero, and Y.-W. Teh. A fast learning algorithm for deep belief nets. *Neural Computation*, 18(7):1527–1554, 2006.

[11] G. B. Huang, M. Ramesh, T. Berg, and E. Learned-Miller. Labeled faces in the wild: A database for studying face recognition in unconstrained environments. Technical Report 07-49, University of Massachusetts, Amherst, October 2007.

[12] T. Jebara. *Discriminative, generative and imitative learning*. PhD thesis, Massachusetts Institute of Technology, 2001.

[13] D. P. Kingma, S. Mohamed, D. Jimenez Rezende, and M. Welling. Semi-supervised learning with deep generative models. In Z. Ghahramani, M. Welling, C. Cortes, N. Lawrence, and K. Weinberger, editors, *Advances in Neural Information Processing Systems 27*, pages 3581–3589. Curran Associates, Inc., 2014.

[14] D. P. Kingma, S. Mohamed, D. J. Rezende, and M. Welling. Semi-supervised learning with deep generative models. In *Advances in Neural Information Processing Systems*, pages 3581–3589, 2014.

[15] D. P. Kingma and M. Welling. Auto-encoding variational Bayes. *International Conference on Learning Representations*, 2014.

[16] N. Kumar, A. C. Berg, P. N. Belhumeur, and S. K. Nayar. Attribute and simile classifiers for face verification. In *International Conference on Computer Vision*, pages 365–372. IEEE, 2009.

[17] M. Mirza and S. Osindero. Conditional generative adversarial nets. *arXiv preprint arXiv:1411.1784*, 2014.

[18] A. Y. Ng and M. I. Jordan. On discriminative vs. generative classifiers: A comparison of logistic regression and naive bayes. In T. Dietterich, S. Becker, and Z. Ghahramani, editors, *Advances in Neural Information Processing Systems 14*, pages 841–848. MIT Press, 2002.

[19] J. Ngiam, A. Khosla, M. Kim, J. Nam, H. Lee, and A. Y. Ng. Multimodal deep learning. In *Proceedings of the 28th international conference on machine learning (ICML-11)*, pages 689–696, 2011.

[20] M. A. Ranzato, F. J. Huang, Y.-L. Boureau, and Y. LeCun. Unsupervised learning of invariant feature hierarchies with applications to object recognition. In *IEEE Conference on Computer Vision and Pattern Recognition*, pages 1–8. IEEE, 2007.

[21] D. J. Rezende, S. Mohamed, and D. Wierstra. Stochastic backpropagation and approximate inference in deep generative models. In T. Jebara and E. P. Xing, editors, *Proceedings of the 31st International Conference on Machine Learning (ICML-14)*, pages 1278–1286. JMLR Workshop and Conference Proceedings, 2014.

[22] R. Salakhutdinov and G. E. Hinton. Deep Boltzmann machines. In *International Conference on Artificial Intelligence and Statistics*, pages 448–455, 2009.

[23] N. Srivastava and R. R. Salakhutdinov. Multimodal learning with deep Boltzmann machines. In *Advances in Neural Information Processing Systems*, pages 2222–2230, 2012.

[24] A. Stuhlmüller, J. Taylor, and N. Goodman. Learning stochastic inverses. In C. Burges, L. Bottou, M. Welling, Z. Ghahramani, and K. Weinberger, editors, *Advances in Neural Information Processing Systems 26*, pages 3048–3056. Curran Associates, Inc., 2013.

[25] V. N. Vapnik. *Statistical learning theory*, volume 1. Wiley New York, 1998.

[26] S. B. Wang, A. Quattoni, L.-P. Morency, D. Demirdjian, and T. Darrell. Hidden conditional random fields for gesture recognition. In *IEEE Conference on Computer Vision and Pattern Recognition*, volume 2, pages 1521–1527. IEEE, 2006.